

## Article

# A Multi-Objective Optimization Method for Single Intersection Signals Considering Low Emissions

Shan Wang <sup>1</sup>, Yu Zhao <sup>1</sup>, Shaoqi Zhang <sup>2,\*</sup>, Dongbo Wang <sup>3</sup>, Chao Wang <sup>3</sup> and Bowen Gong <sup>4,5,\*</sup> 

- <sup>1</sup> Intelligent Transport System (ITS) R & D Center, Shanghai Urban Construction Design and Research Institute (Group) Co., Ltd., Shanghai 200125, China; wangshan@sucdri.com (S.W.); zhaoyu@sucdri.com (Y.Z.)
- <sup>2</sup> China FAW Group Co., Ltd., Changchun 130011, China
- <sup>3</sup> Bureau of Transportation and Construction, TEDA Administrative Commission, Tianjin 300450, China; wangdb@teda.gov.cn (D.W.); wangchao87@163.com (C.W.)
- <sup>4</sup> Department of Traffic Information and Control Engineering, Jilin University, Changchun 130022, China
- <sup>5</sup> Jilin Engineering Research Center for Intelligent Transportation System, Changchun 130022, China
- \* Correspondence: zsq21@mails.jlu.edu.cn (S.Z.); gongbowen@jlu.edu.cn (B.G.)

**Abstract:** The exponential growth of urban centers has exacerbated the prevalence of traffic-related issues. This surge has amplified the conflict between the escalating need for travel among individuals and the constricted availability of road infrastructure. Consequently, the escalation of traffic accidents and the exacerbation of environmental pollution have emerged as increasingly pressing concerns. Urban road intersections, serving as pivotal junctures for vehicle convergence and dispersal, have remained a focal point for scholarly inquiry regarding enhanced operational efficacy and safety. Concurrently, vehicles navigating intersections are subject to external influences, such as pedestrian crossings and signal controls, causing frequent fluctuations in their operational dynamics. These fluctuations contribute to heightened exhaust emissions, exacerbating air pollution and posing health risks to pedestrians frequenting these intersections. A reasonable signal timing scheme can enable more vehicles to pass through the intersection safely and smoothly and reduce the pollutants generated by transportation. Therefore, optimizing signal timing schemes at intersections to alleviate traffic problems is a topic that needs to be studied urgently. In this paper, the emission model based on specific power is analyzed. Through an analysis of the correlation between specific power distribution intervals and the emission rates of individual pollutants, it has been observed that vehicle emission rates are at their lowest during idle speed, progressively increasing with rising vehicle speeds. Investigation into specific power distribution based on variables, such as vehicle type, frequency of stops, and varying delays, has led to the deduction that the peak specific power of vehicles at intersections consistently occurs within the (0, 1) interval. Furthermore, it has been established that high-saturation intersections exhibit higher peak specific power compared to low-saturation intersections.

**Keywords:** single intersection; traffic signal timing; traffic emissions; multi-objective optimization; improved genetic algorithms



check for updates

**Citation:** Wang, S.; Zhao, Y.; Zhang, S.; Wang, D.; Wang, C.; Gong, B. A Multi-Objective Optimization Method for Single Intersection Signals Considering Low Emissions. *Sustainability* **2024**, *16*, 3522. <https://doi.org/10.3390/su16093522>

Academic Editor: Armando Carteni

Received: 6 March 2024

Revised: 17 April 2024

Accepted: 19 April 2024

Published: 23 April 2024



**Copyright:** © 2024 by the authors. Licensee MDPI, Basel, Switzerland. This article is an open access article distributed under the terms and conditions of the Creative Commons Attribution (CC BY) license (<https://creativecommons.org/licenses/by/4.0/>).

## 1. Introduction

The rapid pace of economic development has brought about a significant increase in the number of vehicles on our roads, drawing considerable attention. The congestion on roads and the increase in vehicle emissions have become issues worthy of attention. A collaborative report [1] titled 2022 Annual Traffic Analysis of Major Chinese Cities, crafted by authoritative institutions, meticulously scrutinized the traffic dynamics across 50 medium-to-large cities nationwide. The thorough analysis of data unearthed a persistent annual upsurge in the travel delay index during peak hours. The urban road intersection is an important node in the traffic network, and traffic participants are numerous. When the vehicle passes through the intersection, the rules of road priority and the control of traffic

lights will produce frequent deceleration, idling, acceleration, and constant speed form of state change. Different driving conditions produce different emissions [2]. Scientific inquiries [3] have unequivocally illustrated that, during vehicular acceleration, the average emissions of hydrocarbons and carbon dioxide soar to levels nearly five times higher than those of their idling counterparts. Similarly, emissions of nitrogen oxides and carbon monoxide surge to levels nearly ten times greater than observed during idle periods. However, traditional intersection signal timing only considers delay and queue length and ignores the impact of emissions [4]. Therefore, this paper proposes a signal timing optimization scheme considering vehicle emissions at intersections. It aims to bridge the gap between traditional approaches to traffic management and the realization of sustainable urban road traffic systems. Firstly, the evaluation index of single-intersection signal control was selected and analyzed, and then a multi-objective evaluation model was constructed. Secondly, the improved genetic algorithm is used to solve the optimal timing scheme model. Finally, the effect is verified by experiments.

The main contributions of this research can be summarized as follows:

- (1) A comprehensive evaluation index system considering emissions is proposed.
- (2) A vehicle emission model based on specific power is proposed.
- (3) The genetic algorithm has been improved to solve the objective function.

The remainder of this paper is organized as follows: Section 2 reviews related research on influencing factors for vehicle emissions, vehicle emission models, and signal control considering vehicle emissions. Section 3 presents the method of signal optimization considering low emissions. In Section 4, experiments are conducted to illustrate the performance of the proposed method. Section 5 concludes the paper with a summary and discusses future work.

## 2. Related Works

With growing environmental awareness, an increasing number of transportation scholars take vehicle emissions into account on traffic signal control optimization [5–7]. This involves three key aspects. Firstly, factors affecting emissions at intersections are analyzed. Secondly, estimation methods for vehicle emissions at intersections are explored. Thirdly, emissions as an optimization target in signal timing and traffic organization are considered.

Vehicle emissions are the results of multi-factor interactions. Research on these vehicular emission factors varies, but the influencing factors of vehicle emissions in the literature differs significantly according to the research content [8]. Data are abundant and include values for the vehicular operating factors and road environmental factors [9]. Vehicle operating factors are mainly divided into fuel-related factors and speed-related factors. Fuel-related factors are dominated by vehicle characteristics and take into account the operational requirements during the vehicle's operation, including the fuel type, fuel consumption, travel distance, and engine type [10,11]. Vehicle running speed is the basic index of emissions in many models, and mainly includes the average speed and instantaneous speed. In the laboratory, various velocity changes are often simulated for emission modeling [12,13].

Some scholars have realized that external environmental factors in vehicle operation need to be taken into account. Costagliola [14] proposed that the actual road conditions of vehicles during operation had a significant impact on the emission results. Yao [15] utilized VISSIM simulation data and discovered that, the greater the slope of the intersection's approach road, the higher the emission factor for motor vehicles. Studies have shown that changes in the parameters between the tires and road surface can also stimulate the running efficiency of vehicles, thus increasing the impact of vehicle emissions [16,17].

When vehicles are running at intersections, they are controlled by signals and adjust between different operating states, which inevitably affects the engine's operating efficiency. Pandian [18] compared CO<sub>2</sub> emissions at an intersection before and after its conversion from signal control to a roundabout. The study found that vehicles' emissions

at roundabouts were lower than at signal-controlled intersections and the difference was statistically significant. Haydari [19], using deep learning and neural networks to optimize intersection signal control, found that travel time is highly correlated with CO<sub>2</sub> emissions and fuel consumption.

There are two main types of intersection vehicle emission models: fuel-based [20,21] and speed-bases [13,22]. Fuel-based emission models are mainly applied to the measurement and analysis of transportation carbon emissions in cities, regions, and whole countries [23]. Applying emission models based on vehicle speed and related parameters is more commonly used at an intersection. Gao [24] categorized queuing vehicles at intersections according to different operating conditions, used fixed acceleration/deceleration values, calculated intersection stop frequencies and delays, and utilized an emission model based on specific power distribution to simplify the calculation of total emissions when vehicles queue in front of signal intersections. Sun [25] referred to the establishment principles of existing emission models, first identified initial emission factors, then adjusted parameters based on influencing factors, and finally combined the two to calculate the emissions. Using available emission data and simulated vehicle operation data, Sun established an emission estimation method for signal intersections under vehicle–road coordination, keeping the relative error between the model results and simulation values within 3%. Xu [26] collected floating vehicle GPS data, clustered specific powers based on the particle swarm algorithm, established a speed-based operation mode distribution model, and compared emission rates for different operation modes, with an error of less than 6.08% against actual values.

Based on emission method research, numerous scholars have analyzed factors influencing emissions and conducted signal optimization research targeting emission reduction at intersections [26,27]. Ba [28] built a simulation platform integrating VISSIM and MOVES to estimate intersection emissions, analyzing the effects of traffic organization optimization, the establishment of left-turn waiting areas, and signal optimization on intersection emissions. Wu [29] found that intersections with borrowed left-turn schemes showed reduced vehicle pollutant emissions, and signal control optimization also decreased emissions. Qu [30] performed regression analysis on emissions and delays, establishing a relationship and developing a signal optimization model targeting emission reduction and delay reduction. Simulation of typical intersections showed a 10.54% reduction in delays and a 13.41% reduction in emissions post-optimization. Li [31] categorized vehicle operating states at intersections into uniform speed, deceleration, idling, and acceleration, providing simplified emission calculation formulas for each state and establishing an emission-minimizing single-point and arterial signal optimization model.

In conclusion, both domestic and international researchers have conducted in-depth on-going studies on traffic signal optimization. However, most researchers, when optimizing traffic signals at single intersections or along arterial roads, tend to rely solely on mobility metrics, with only a few incorporating sustainability metrics. Among those who use sustainability metrics, many rely on specific power models, using tools like MOVES to establish emission calculation platforms for intersection vehicle emissions. However, such methods have not quantified the relationship between signal timing parameters, evaluation metrics, and emissions, making it difficult to analyze the quantitative impact of signals on emissions.

Hence, this paper aims to overcome these limitations by quantifying the relationship between signal timing parameters, evaluation metrics, and emissions. It integrates both mobility and sustainability metrics for signal optimization at single intersections. The aim is not only to alleviate congestion and optimize signal timings but also curtail environmental ramifications by intelligently addressing emissions during peak traffic hours. Through a comprehensive analysis of intersection-based emissions patterns, this research aspires to contribute substantively to the development of sustainable urban road traffic systems.

### 3. Materials and Methods

#### 3.1. Evaluation Metrics for Single-Intersection Signal Control

Urban intersection signal control can temporally segregate the flow of traffic, reduce conflict points, enhance traffic safety, and ensure optimal throughput and environmental benefits when traffic signals are allocated reasonably. This section introduces commonly used optimization indicators for intersection signals: mobility metrics (throughput capacity, delay time, and queue length) and sustainability metrics (pollutant emissions).

##### 3.1.1. Throughput Capacity of the Intersection

The throughput capacity of an intersection depends on its geographical environment, channelization shapes, and signal timings. It represents the maximum traffic volume passing through the road's approach in a unit time under specific conditions and is a crucial metric for assessing the fluidity of an intersection. The throughput can vary due to differences in signal control methods, intersection geometrical structures, traffic participation conditions, and other factors. The calculation method is as shown in Formula (1):

$$\text{Cap} = S \cdot \frac{g_e}{C} = S \cdot u \quad (1)$$

where:

S is the saturation flow rate of the approach, unit: pcu/h (passenger car units per hour);

$g_e$  is the effective green light time of the phase, unit: s (seconds);

C is the signal cycle duration, unit: s (seconds);

u is the green signal ratio of the signal phase, dimensionless;

Cap is the throughput capacity of the signalized intersection, unit: pcu/h (passenger car units per hour).

##### 3.1.2. Delay at the Intersection

Delay time is one of the most frequently used metrics to assess the operational status of an intersection. The severity of congestion at an intersection is directly proportional to the average delay time experienced by vehicles operating there. Conversely, a smaller average delay time indicates smoother vehicle flow. The delay time consists of four main components: delay caused by signal control, delay due to vehicle queuing, delay arising from vehicle braking, and delay resulting from vehicle lane changing.

Popular models for calculating delay at intersections include the HCM (Highway Capacity Manual) model [32], the steady-state theory [33], and the fixed number theory [34]. Given that the steady-state theory and the constant theory are too idealistic in their conditions, in the actual operation of intersections vehicle departures and arrivals function discretely. The HCM model divides vehicle delay at intersections into random delay and average delay. Random delay is caused by uneven traffic volume arrivals during different cycles of the intersection, leading to imbalances in certain periods and resulting in longer queues. Average delay occurs when the vehicle arrival rate remains constant or changes very little. By integrating the steady-state theory [33] and the constant theory [34], the HCM model can be improved. The formula is as follows:

$$\tilde{d}_{all} = \frac{\sum_{i=1}^n q_i \cdot \tilde{d}_i}{\sum_{i=1}^n q_i} \quad (2)$$

$$\tilde{d}_i = \frac{q_i}{2u_i S_i (u_i S_i - q_i)} + \frac{1 - u_i}{2q_i} + \frac{C(1 - u_i)^2}{2(1 - y_i)} \quad (3)$$

where:

$\tilde{d}_{all}$  is the total delay within the intersection's cycle, unit: s (seconds);

$\tilde{d}_i$  is the average delay of vehicles during the  $i$ th phase of the intersection's cycle, unit: s (seconds);

$q_i$  is the traffic volume during the  $i$ th phase of the intersection's cycle, unit: pcu/h (passenger car units per hour).

### 3.1.3. Vehicle Queue Length at the Intersection

The maximum queue length represents the greatest distance between the stop line of the approach and the rearmost vehicle within a single cycle. If this length exceeds the distance to the preceding intersection, it may lead to overflow queuing, significantly hindering the signal control effectiveness of the upstream intersection. When the intersection is in an oversaturated state, there is a possibility of intersection "spillover", where vehicles from the previous cycle queue up to the upstream intersection, obstructing the normal traffic flow of the upstream intersection. The queue length of vehicles at this intersection can be calculated using Formula (4).

$$l = \frac{Q}{4} \left[ \sqrt{\frac{12(x - x_0)}{u \cdot C} + (x - 1)^2} - 1 + x \right] \quad (4)$$

where:

$$x_0 = \frac{t_g q_s}{600} + 0.67 \quad (5)$$

where:

$l$  is the queue length of vehicles when the green light just turns on at the start of the cycle at the intersection, unit: m (meters);

$Q$  is the throughput capacity of the intersection, unit: pcu/h (passenger car units per hour);

$u$  is the green signal ratio of the signal phase, dimensionless;

$x$  is the saturation degree of the intersection, dimensionless;

$C$  is the cycle of the intersection, unit: s (seconds);

$q_s$  is the saturation flow rate of the approach at the intersection, unit: pcu (passenger car units).

When the saturation degree of the intersection approaches 1, the queue length is:

$$l = T_{red}q + t_g \cdot (q - u) + l_s \quad (6)$$

where:

$l_s$  represents the queue length of vehicles left over from the previous cycle at the intersection, unit: m.

$q$  represents the vehicle arrival rate, unit: pch/h.

$u$  is the green signal ratio for the signal phase, dimensionless.

$T_{red}$  stands for the red light at the intersection phase, unit: S.

When the intersection is in an under-saturated state, the queued vehicles consist of those arriving during the red light and those left over and not entering the intersection before the red light starts. The queue length can be calculated using Equation (7):

$$l = l_{start} + l_{red} \quad (7)$$

where:

$$l_{start} = \frac{\exp \left[ -\frac{4(1-x)}{3x} \cdot (q_s \cdot C \cdot u)^{\frac{1}{2}} \right]}{2(1-x)} \quad (8)$$

$$l_{red} = q \cdot T_{red} \quad (9)$$

where:

$l_{start}$  is the queue length of vehicles remaining at the intersection after the green light ended in the previous cycle, unit: m.

$l_{red}$  is the queue length of vehicles arriving at the intersection during the red-light duration, unit: pch/h.

### 3.1.4. Vehicle Emission at the Intersection

In recent years, topics like “carbon neutrality” and “carbon peak” have gradually become parts of our daily lives. This has prompted traffic management departments to elevate the control of vehicle exhaust emissions to the same importance level as intersection traffic efficiency. Reducing vehicle exhaust emissions while increasing the efficiency of intersections, such as by decreasing delays and queue lengths, is an urgent problem that we need to address.

When calculating pollutant emissions at an intersection, one can sum up the cumulative emissions of individual vehicles. The emission of a single vehicle passing through the intersection is shown in Equation (10):

$$TE = \sum_{i=1}^m \sum_{j=1}^n E_{ij} \cdot fVSP_i \quad (10)$$

where:

$i$  is the power ratio interval index.

$j$  is the pollutant category.

$E_{ij}$  is the emission rate of pollutant category  $j$  in the power ratio interval  $i$ .

$fVSP_i$  is the number distribution of the vehicle’s instantaneous power ratio in power ratio interval  $i$ .

Once the per-second pollutant emission of a single vehicle is obtained, the total emissions at the intersection can be calculated. The overall emissions at the intersection can be calculated by dividing into approach road sections. The total emissions for each approach road section can be further divided into emissions due to vehicle waiting time at the intersection and emissions from vehicles passing through the intersection. The calculation formula is shown below:

$$AE_k^1 = TE \cdot q_k \cdot (L_k - l_k) \quad (11)$$

$$AE_k^2 = \frac{1}{3600} (TE \cdot q_k \cdot D_k) \quad (12)$$

where:

$k$  is the approach road section. Typically, there are four for a cross intersection and three for a T-shaped intersection.

$AE_k^1$  is the emission amount from vehicles passing through the intersection in the  $k^{\text{th}}$  approach road section.

$AE_k^2$  is the emission amount from vehicles waiting at the intersection in the  $k^{\text{th}}$  approach road section.

$L_k$  is the length from the upstream intersection to the stop line of the  $k^{\text{th}}$  approach road section at the intersection, unit: m.

$D_k$  is the average delay time per vehicle in the  $k^{\text{th}}$  approach road section at the intersection, unit: s/pcu.

Therefore, the total pollutant emissions for the entire intersection can be expressed as:

$$AE = \sum_k AE_1 + \frac{1}{3600} \sum_k AE_2 \quad (13)$$

where:

$AE$  is the total emission amount at the intersection, with the unit: g.

Substituting Equations (11) and (12) into Equation (13) gives:

$$AE = \sum_k [TE \cdot q_k \cdot (L_k - l_k)] + \frac{1}{3600} \sum_k [TE \cdot q_k \cdot D_k] \quad (14)$$

After selecting and analyzing the indicators for single-intersection signal timing evaluation, we need to establish a multi-objective evaluation model to improve the efficiency of intersections and reduce pollutant emissions.

### 3.2. Construction of the Multi-Objective Optimization Model for Single-Point Intersections

#### 3.2.1. Construction of the Multi-Objective Optimization Function

The main goal of this paper is to establish a multi-objective optimization model to improve the efficiency of the intersection and reduce pollutant emissions. Thus, the optimization objectives are to minimize the overall pollutant emissions of the intersection, minimize delay time, and minimize the queue length. A multi-objective optimization model for signal timing at a single-point intersection is constructed. The objective function is shown in Equation (15):

$$\min \frac{\tilde{d}_{opt}}{\tilde{d}_{ori}}, \frac{l_{opt}}{l_{ori}}, \frac{AE_{opt}}{AE_{ori}} \quad (15)$$

where:

$\tilde{d}_{opt}$  is the average vehicle delay after optimizing the signal timing scheme at the intersection, unit: s.

$\tilde{d}_{ori}$  is the average vehicle delay of the original signal timing scheme at the intersection, unit: s.

$l_{opt}$  is the average queue length after optimizing the signal timing scheme at the intersection, unit: m.

$l_{ori}$  is the average queue length of the original signal timing scheme at the intersection, unit: m.

$AE_{opt}$  is the pollutant emission amount after optimizing the signal timing scheme at the intersection, unit: g.

$AE_{ori}$  is the pollutant emission amount of the original signal timing scheme at the intersection, unit: g.

The results of the multi-objective optimization function can only be on the Pareto frontier, making it impossible to find a solution that optimally satisfies every individual objective function. Given that the three current objective functions are dimensionless, we can multiply them together, converting them into a single objective function. The optimal solution can then be obtained, as shown in Equation (16).

$$\min \frac{\tilde{d}_{opt}}{\tilde{d}_{ori}} \times \frac{l_{opt}}{l_{ori}} \times \frac{AE_{opt}}{AE_{ori}} \quad (16)$$

According to Equation (16), we need to find an optimal solution that minimizes the overall value. Converting multi-objectives into a single objective function is more reasonable than the simple weighted allocation method because the latter requires considering the weight of each objective and is highly subjective.

#### 3.2.2. Multi-Objective Optimization Model at a Single Point Intersection

During the optimization process of the signal timing scheme at a single-point intersection, the optimal solution obtained solely based on the objective function often cannot be applied in practice. Constraints are usually added to variables based on real-world conditions. Considering the traffic environment conditions and road parameters, the following constraints are applied:

##### (1) Degree of Saturation

The signal timing at intersections is significantly influenced by the degree of saturation; thus, its value should neither be too high nor too low. The researchers explored the relationship between saturation and delays [35] to determine the critical saturation values that are appropriate for the actual situation and for congestion. When saturation levels

exceed 0.85, this indicates that the intersection is oversaturated. In this state, the volume of traffic exceeds the intersection's capacity to efficiently handle it. Conversely, when saturation levels fall below 0.6, this indicates that the intersection is operating below its capacity. While traffic may flow smoothly under these conditions, the intersection is not maximizing its potential throughput, resulting in underutilization of resources. In such scenarios, applying complex multi-objective optimization schemes for signal timing may not yield substantial benefits. This is because the intersection is not facing significant congestion issues that necessitate intricate optimization strategies. Therefore, based on the actual operating conditions of the intersection, constraints on the degree of saturation for a single-point signal-controlled intersection are applied as follows:

$$0.6 < x < 0.85 \quad (17)$$

## (2) Green Light Duration

In urban single-point intersection signal control, the green light duration of each phase is a crucial indicator affecting the intersection's traffic efficiency. It is closely related to the waiting time and queue length of vehicles and pedestrians at the intersection, as well as the smoothness of the traffic flow. If the green light duration at an intersection is too short, it may prevent slower pedestrians from crossing the intersection safely. Moreover, it could lead to frequent switching of traffic lights, causing vehicles to frequently start and stop at the intersection, exacerbating pollutant emissions and increasing delay times. If the green light duration is too long, there might be instances of idling, increasing the waiting time for other phases in red. This can cause agitation among drivers and potentially increase the likelihood of accidents. Therefore, it is essential to specify maximum and minimum values for the green light duration of each phase. The green light duration of each phase at a single-point intersection can be constrained using Equation (18).

$$g_{min} \leq g_i < g_{max} \quad (18)$$

where:

$g_i$  is the green light duration of the  $i^{\text{th}}$  phase at the intersection, unit: s.

$g_{min}$  is the minimum green light duration of the  $i^{\text{th}}$  phase at the intersection, unit: s.

$g_{max}$  is the maximum green light duration of the  $i^{\text{th}}$  phase at the intersection, unit: s.

## (3) Signal Cycle Duration

The signal cycle duration of a signal-controlled intersection is another factor affecting its traffic efficiency. A cycle that is either too long or too short can negatively impact not just the intersection but potentially the efficiency of the entire road network. Therefore, it is essential to apply constraints to the intersection's signal cycle duration, as shown in Equation (19), ensuring that the optimized cycle duration aligns with the road's actual conditions.

$$C_{min} \leq C < C_{max} \quad (19)$$

where:  $C$  is the cycle duration of the intersection, unit: s.  $C_{min}$  is the minimum cycle duration of the intersection, unit: s.  $C_{max}$  is the maximum cycle duration of the intersection, unit: s.

Based on the previously presented multi-objective optimization function for signal timing, along with its three constraints, the multi-objective optimization model at a single point intersection can be established as shown in Equation (20).

$$F = \min \left[ \frac{\tilde{d}_{opt}}{\tilde{d}_{ori}} \times \frac{l_{opt}}{l_{ori}} \times \frac{AE_{opt}}{AE_{ori}} \right] \text{ s.t. } \begin{cases} 0.6 < x < 0.85 \\ g_{min} \leq g_i < g_{max} \\ C_{min} \leq C < C_{max} \end{cases} \quad (20)$$

After the multi-objective optimization model at a single point intersection is built, the model needs to be solved to obtain the optimal solution.

### 3.3. Optimization Model Solution Based on Genetic Algorithms

Genetic algorithm (GAs) [36] are a type of modern optimization algorithm. According to the law of survival of the fittest in nature, the genes of the superior individuals in the population are inherited. The chromosomes of each individual produce new chromosomes with greater fitness through the process of selection, crossover and mutation, among which the individuals with greater fitness are favourable for selection, the population is optimized, the solution approximation is close to the optimal solution, and the population is continuously optimized by repeated iterations to finally obtain the optimal solution to the target problem. GAs are an intelligent search algorithm based on the principles of natural selection and genetic mechanisms.

GAs generate initial points randomly, facilitate parallel searches, and operate in encoded forms, minimizing impact on the decision variables themselves. Operations, like selection and mutation, generate newer, more optimal individuals and populations. After multiple iterations, the best-performing individual is obtained, representing the optimal solution to the optimization problem. With a broader operational space, the algorithms only need a fitness function for evaluations. The iterative process is probability-driven, ensuring efficient and effective global optimization. Given these advantages, this paper adopts the GA as the solution for the single-point intersection signal control optimization model.

#### 3.3.1. Implementation Steps of GAs

The computational flowchart of the genetic algorithm is shown in Figure 1.

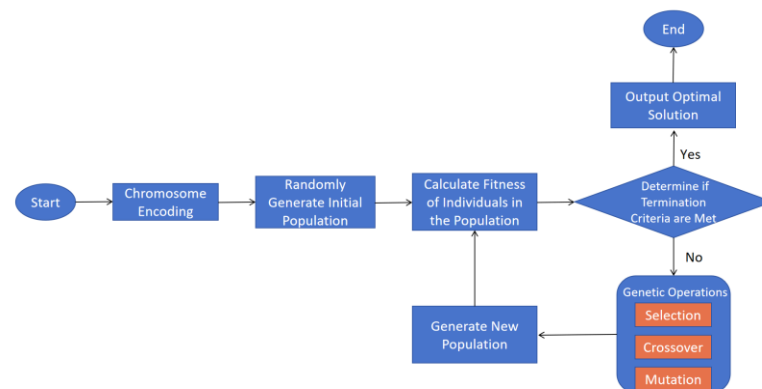


**Figure 1.** Flowchart of Genetic Algorithm Principal Calculation.

#### Step 1: Chromosome Gene Encoding

In genetic algorithms, individuals in a population have the same number of chromosomes, each representing optimization parameters, like cycle duration and green signal ratio, for a single-point signal-controlled intersection. Genes on chromosomes encode these parameters, with different combinations, yielding varying fitness levels. Chromosomes are passed to the next generation through individual mating.

#### Step 2: Random Generation of Initial Population

The initial population size ( $N$ ) in genetic algorithms must be carefully chosen. If it is too small, the algorithm's optimization potential is limited, possibly hindering optimal solution identification. Conversely, if  $N$  is too large, although the likelihood of finding optimal fitness increases, it can decrease optimization efficiency, consuming more time. Therefore, the initial population size should be chosen based on the computational capabilities of the hardware.

#### Step 3: Calculate the Fitness of Individuals within the Population

When the genetic algorithm solves the objective function, fitness is used as the criterion to evaluate the effect. Higher fitness means better traits. Our objective function, on the other hand, needs to be as low as possible for each indicator, so we need to convert the

objective function into fitness. We take fitness as the reciprocal of the objective function, as shown in Equation (21).

$$f = \frac{1}{F} \quad (21)$$

where  $F$  is the objective function and  $f$  is the fitness function.

#### Step 4: Perform Selection Operator Operation

The selection operator is the most critical part of the genetic operations in a genetic algorithm. We choose roulette wheel selection [37] because the basic idea of this method is that the probability of each individual being selected is directly proportional to its fitness. This method is conducive to the selection of targets with high adaptability in the process of multi-objective optimization and promotes the rapid evolution of genetic algorithms. This can be represented by Equation (22).

$$P_i = \frac{f_i}{\sum_1^N f_i} \quad (22)$$

where:

$N$  represents the population size.

$f_i$  represents the fitness of the  $i^{\text{th}}$  individual, dimensionless.

$P_i$  represents the probability of the  $i^{\text{th}}$  individual being selected during the genetic operation, dimensionless.

#### Step 5: Perform Crossover Operator Operation

In genetic algorithms, the crossover operator mates individuals to create new ones with unique genes. The crossover probability is a crucial parameter, balancing precision and diversity. High probabilities ensure enough offspring but may compromise precision, while low probabilities risk premature convergence. A piecewise function is needed: early stages favor high probabilities for diversity, later stages decrease them for precision. The crossover probability can be calculated using Equation (23).

$$P_{jc} = \begin{cases} P_{jcmax} - \frac{(f' - f_a)(P_{jcmax} - P_{jcmin})}{f_{max} - f_a} & f' \geq f_a \\ P_{jcmin} & f' \leq f_a \end{cases} \quad (23)$$

where:

$P_{jcmax}$  is the user-defined maximum crossover probability for the population, dimensionless.

$P_{jcmin}$  is the user-defined minimum crossover probability for the population, dimensionless.

$f'$  is the higher fitness value between the two individuals undergoing crossover in the population, dimensionless.

$f_a$  is the average fitness of the current generation in the population, dimensionless.

$f_{max}$  is the maximum fitness of the current generation in the population, dimensionless.

#### Step 6: Perform Mutation Operator Operation

In genetic algorithms, the mutation operator simulates gene mutation, enhancing population diversity and global search capabilities. The mutation probability is crucial. High probabilities risk instability due to excessive mutations, making it hard to find optimal solutions. Low probabilities limit search capabilities, hindering convergence. Balancing mutation probability is vital for effective optimization. Therefore, similar to the crossover operator, the mutation operator also requires a piecewise nonlinear function, as shown in Equation (24).

$$P_{by} = \begin{cases} P_{bymax} - \frac{(f_{max} - f')(P_{bymax} - P_{bymin})}{f_{max} - f_a} & f' \geq f_a \\ P_{bymin} & f' \leq f_a \end{cases} \quad (24)$$

where:

$P_{bymax}$  is the user-defined maximum mutation probability for the population, dimensionless.

$P_{jmin}$  is the user-defined minimum mutation probability for the population, dimensionless.  
 $f_a$  is the average fitness of the current generation in the population, dimensionless.

Step 7: Determine if the Algorithm Meets the Termination Criteria

Given finite computational resources, termination criteria must be set for genetic algorithms. Two common methods are:

Precision-based: If the optimal solution remains unchanged or varies very slightly for  $x$  consecutive generations, the loop terminates, and the optimal solution is output.

Generation-based: The algorithm evolves for  $Y$  generations, and the optimal solution of the  $Y$ th generation is output. If the termination criteria are met, the algorithm concludes; otherwise, the process repeats until an optimal solution is achieved.

### 3.3.2. Genetic Algorithm Optimization Solution

In genetic algorithms, obtaining the global optimal solution can be challenging due to the standard operators potentially disrupting good gene combinations. To address this, an improved genetic algorithm is proposed. This includes a selection operator aimed at retaining the global optimal solution, crucial for converging multi-objective optimization problems to their global optima.

Step 1: According to the encoding rules, initialize a population  $P$  composed of  $N$  individuals. The population  $P$  can be described as follows:

$$P(t) = \{a_1(t), a_1(t), \dots, a_N(t)\} \quad (25)$$

Step 2: If the stopping condition is met, terminate the process. Otherwise, continue with the following steps.

Step 3: Calculate the fitness of the best individuals in the  $t^{th}$  and  $(t + 1)^{th}$  generations, as follows:

$$f_{max}(t) = \max\{f(a_1(t)), f(a_1(t)), \dots, f(a_N(t))\} \quad (26)$$

$$f_{max}(t+1) = \max\{f(a_1(t+1)), f(a_1(t+1)), \dots, f(a_N(t+1))\} \quad (27)$$

Step 4: Pass all the best individuals from the current population to the next generation. Independently select the remaining  $N - 1$  individuals from the current population, as follows:

if  $f_{max}(t) > f_{max}(t+1)$  then replicate:

$$\{a'_k(t) = \{a_k(t) | f(a_k(t)) > f_{max}(t+1), a_k(t) \in P(t)\}$$

replace the worst ones of  $\{a_j(t+1) \in P(t+1)\}$  with  $\{a'_k(t)\}$

end if

Step 5: Independently perform crossover and mutation operations on the  $N - 1$  individuals. Then, obtain a new generation of the population with  $N$  individuals.

Step 6: Return to Step 2. To verify the effectiveness of the improved genetic algorithm, we compared the fitness calculation results of the standard genetic algorithm and the improved genetic algorithm. The crossover and mutation probabilities for the genetic algorithm were set to 0.5, respectively, the initial population size was set to 1000, and the number of population iterations was set to 50. The final results are shown in Figure 2.

According to Figure 2a, we can observe that the standard genetic algorithm does not guarantee that the fitness of the best individual in the current generation is always better than that of the previous generation. For instance, when evolving from the eighth to the ninth generation, the fitness of the best individual is actually worse than before. On the other hand, the improved genetic algorithm retains the best individual from each generation, as described in Step 4, ensuring they do not participate in crossover and mutation. As a result, it guarantees that the best individual's fitness in the current generation is never less than that of the previous generation. For example, as shown in Figure 2b, the fitness of the population's best individual always increases, indicating that the improved genetic algorithm can be used to find the global optimum for optimization problems.

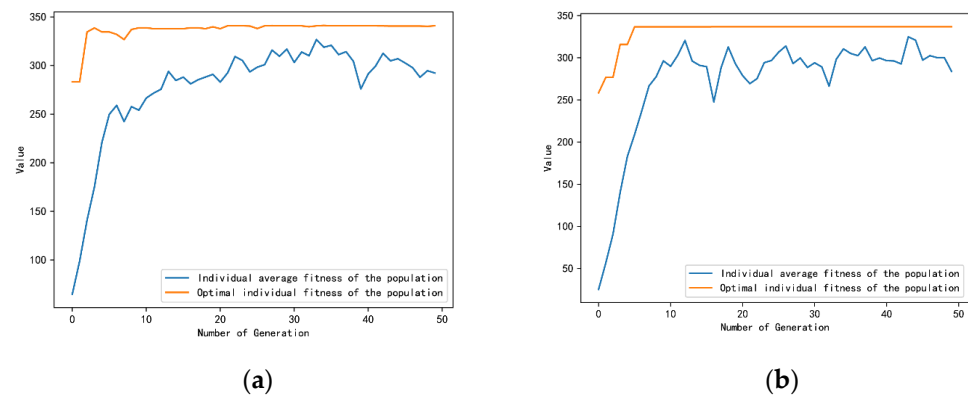


**Figure 2.** Fitness calculation before and after genetic algorithm improvement. (a) Population fitness calculation using the standard genetic algorithm. (b) Population fitness calculation using the improved genetic algorithm.

#### 4. Experiment and Result

##### 4.1. Experimental Setup

This verification example utilizes VISSIM4.3 simulation software, known for accurately replicating real road traffic conditions based on its designed models and parameters. Subsequently, traffic flow conditions and road parameters are input into the single-point intersection signal control multi-objective optimization model. Decision variables from the model are encoded and input into the improved genetic algorithm. Using this algorithm, we can compute the optimal signal timing that satisfies the objective function and constraints. This optimal scheme is then automatically input into the VISSIM signal group via the VISSIM COM interface. Running the VISSIM simulation provides results like the average delay at the intersection, the average queue length, and pollutant emission levels. These results are logged into a file. Within the VISSIM microscopic simulation framework, the optimal signal timing is recalculated every 10 min, implementing rolling optimization for a 24-h period at the intersection. Finally, the simulation outputs are analyzed to validate the effectiveness of the model and algorithm. The system framework based on VISSIM microscopic simulation is shown in Figure 3.

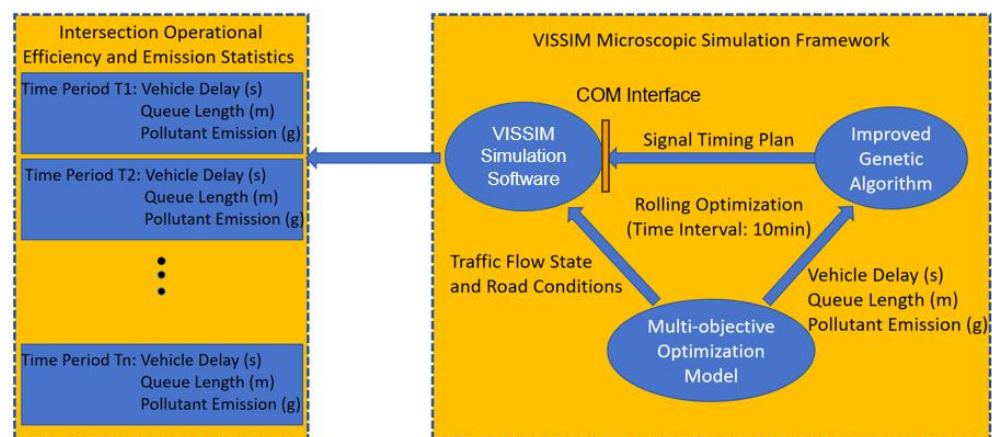


**Figure 3.** System Framework of VISSIM Microscopic Simulation.

##### 4.1.1. Simulation Road Network and Scenario Construction

The intersection of Jinshui Road and Renmin Road in the main urban area of Taiqian County is chosen as the examination scenery. This intersection is a 4-phase junction, equipped with a traffic island. The planar channelization diagram and 3D view are shown in Figure 4.

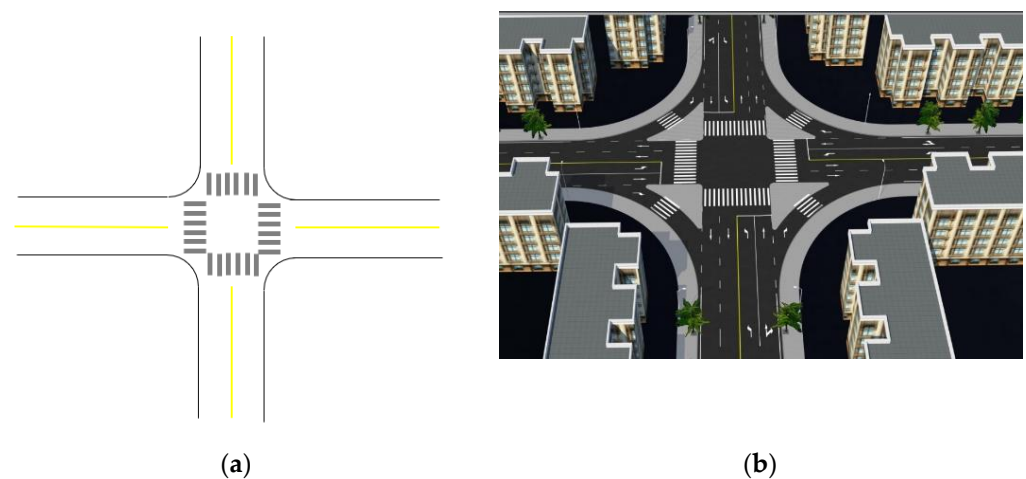


**Figure 4.** Channelization map of Jinshui Road and Renmin Road intersection. (a) Plan view of the intersection. (b) Plan view of the intersection.

Through a traffic survey at the intersection, actual operational data of the junction was obtained.

(1) Signal timing of the intersection

The intersection of Jinshui Road and Renmin Road operates on a fixed signal timing scheme, with a cycle length of 162 s. It is a four-phase intersection. The signal timings for each phase are as shown in Table 1.

**Table 1.** Signal timing at the intersection of Jinsui Road and Renmin Road.

Phase	Direction	Green Light Duration (s)	Red Light Duration (s)	Yellow Light Duration (s)	All-Red Duration (s)	Cycle (s)
Phase 1	East–West Straight Through	46	101	3	3	162
Phase 2	East–West Left Turn	30	117	3	3	162
Phase 3	North–South Straight Through	47	100	3	3	162
Phase 4	North–South Left Turn	26	121	3	3	162

(2) Traffic Volume Survey at the Intersection

The traffic flow survey was conducted at the same time on 12 December 2021 and 13 December 2021, from 16:40 to 17:40, with an hourly interval. The survey method was aerial photography using drones. At the intersection, statistics were gathered from both the flow volume of each incoming lane and the flow volume of each incoming direction. The number of vehicles recorded from the survey is shown in Table 2.

**Table 2.** Traffic Volume at the Intersection.

Entry/Flow Direction	Left Turn	Right Turn	Straight Through
East Entry	312	329	572
West Entry	410	525	309
North Entry	538	535	202
South Entry	532	457	341

Based on the survey results of the example scenario provided above, a VISSIM simulation network was constructed, as shown in Figure 5.

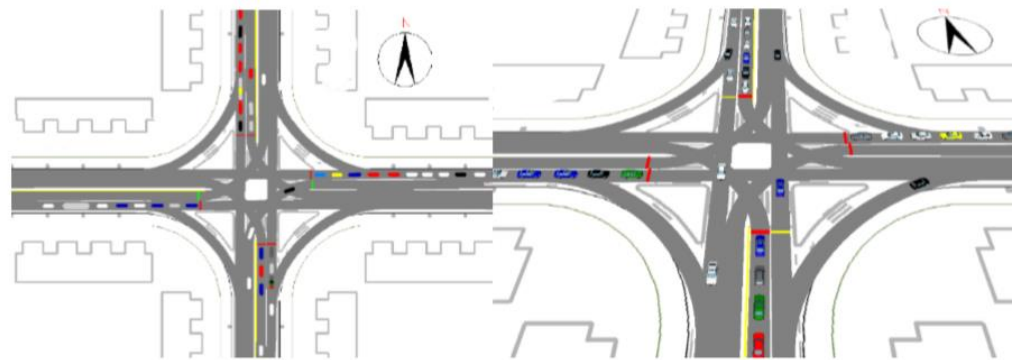


**Figure 5.** VISSIM Simulation Diagram of the Jinshui Road and Renmin Road Intersection (Current Situation).

#### 4.1.2. Calibration of Model and Algorithm Parameters

##### (1) Calibration of signal timing parameters

During the optimization process of the intersection signal timing, it is necessary to calibrate the parameters used. Specific parameter calibration is shown in Table 3.

**Table 3.** Calibration of Intersection Signal Timing Parameters.

Start-Up Loss Time	Yellow Light Duration	All-Red Duration	All-Red Duration
$\frac{a+b}{2}$	$\frac{T_y}{2}$	$\frac{T_R}{0}$	$\frac{L = a + b + T_y}{4}$

##### (2) Green light duration constraint

Ensuring the safe crossing time for pedestrians in each direction at the intersection is also something to consider during signal optimization. This paper adopts the minimum green light duration calculation formula for pedestrian safe crossing proposed by HCM2010, as shown in Formula (28).

$$g_{min} = \begin{cases} 3.2 + \frac{l_{person}}{v_{person}} + 0.81 \frac{N_{person}}{w_{person}}, & w_{person} > 3.0 \\ 3.2 + \frac{l_{person}}{v_{person}} + 0.27 \frac{N_{person}}{w_{person}}, & w_{person} \leq 3.0 \end{cases} \quad (28)$$

where:

$g_{min}$  is the shortest green light duration allocated for the  $i$ th phase at the intersection, measured in seconds (s);

$l_{person}$  is the length of the pedestrian crosswalk at the intersection, measured in meters (m);

$w_{person}$  is the width of the pedestrian crosswalk at the intersection, measured in meters (m);

$v_{person}$  is the speed of pedestrians crossing the intersection, measured in meters per second (m/s);

$N_{person}$  is the number of people crossing the intersection during one cycle.

The designed saturation constraint for the intersection is:  $0.6 < x < 0.85$ . Based on the saturation constraint and the minimum green light duration for pedestrian safety, the green light duration constraint range for each phase at the intersection can be calculated, as shown in Table 4.

**Table 4.** Green light duration constraints for each phase at the intersection.

Green Light Phase	Minimum Green Light Duration	Maximum Green Light Duration
Phase 1	20 s	65 s
Phase 2	30 s	70 s
Phase 3	20 s	65 s
Phase 4	30 s	70 s

- (3) Lane Saturation Flow Rate. To more accurately calculate the saturation flow rate of a certain incoming lane composition, corrections are made for right-turn and left-turn traffic flows, as shown in Equations (29) and (30).

$$f_{RT} = \begin{cases} 0.8, & \text{Right Turn Only Lane} \\ 1.0 - 0.2V_{RT}, & \text{Straight-Right Combined Lane} \\ 1.0 - 0.25V_{RT}, & \text{Left-Straight-Right Combined Lane} \end{cases} \quad (29)$$

where:  $f_{RT}$  is the right-turn correction factor.  $V_{RT}$  is the proportion of right-turn traffic flow.

$$f_{LT} = \begin{cases} 0.8, & \text{Left Turn Lane with Dedicated Left Turn Phase} \\ \frac{1}{1.0+0.2V_{LT}}, & \text{Straight-Left Combined Lane} \end{cases} \quad (30)$$

where:  $f_{LT}$  is the left-turn correction factor.  $V_{LT}$  is the proportion of left-turn traffic flow.

In accordance with the HCM 2010 method for lane saturation flow rates, along with lane correction factors, the calculated saturation flow rates for left-turn, right-turn, and through lanes are 1200 veh/h, 1000 veh/h, and 1500 veh/h, respectively.

- (4) Parameters of the Improved Genetic Algorithm

In this paper, an improved genetic algorithm is employed to solve the multi-objective optimization model, and the parameters used during the algorithm's execution are calibrated, as shown in Table 5.

**Table 5.** Calibration of Genetic Algorithm Parameters.

Parameter	Calibrated Value
Maximum Evolution Generations	50
Maximum Crossover Probability	0.5
Minimum Crossover Probability	0.1
Maximum Mutation Probability	0.5
Minimum Mutation Probability	0.05
Population Size	100

#### 4.2. Result and Discussion

This paper presents the implementation of a model using Python, with the genetic algorithm utilizing the third-party library *geatpy*. Computation tasks were performed on a desktop computer equipped with an Intel® Core™ i5-9400 (2.9GHz) CPU (Intel, Santa Clara, CA, USA). The computed results were then interfaced with the signal timing controller of VISSIM via its COM interface. The VISSIM simulation duration was set to 3600 s, with signal timing optimization conducted every 600 s. The random seed used for the computations was 44. The optimization results obtained throughout the 3600 s of VISSIM simulation are presented in Table 6.

Table 6 outlines the optimization scheme iterations along with their respective execution times. It is notable that the algorithm consistently converged towards improved signal timing plans, showcasing its effectiveness in enhancing traffic flow efficiency. However, while the execution times remained relatively consistent across iterations, there may be scope for further optimization to reduce computational overhead, especially for real-time applications or large-scale traffic networks.

**Table 6.** Genetic Algorithm Solving Results.

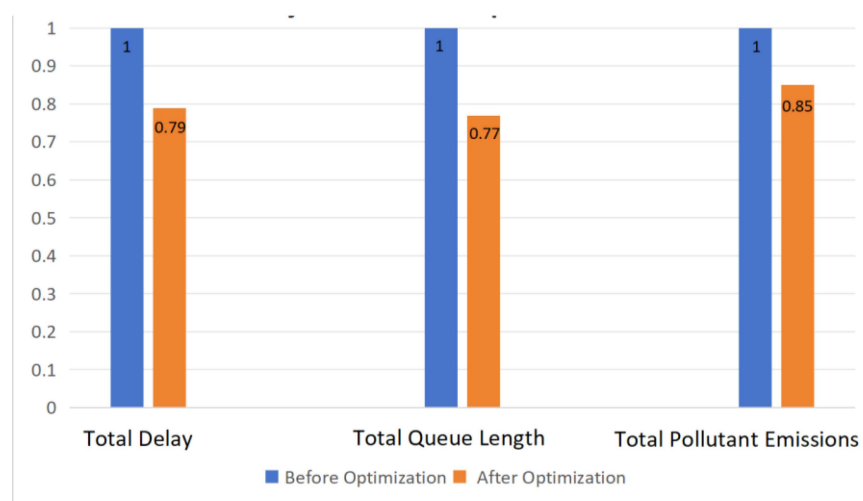
Optimization Iteration	Time Instant	Optimization Scheme	Program Execution Time
0	0	[48, 30, 48, 27, 165]	(Initial Moment) 0
1	600 s	[51, 40, 32, 35, 170]	3.75 s
2	1200 s	[42, 31, 37, 48, 170]	4.13 s
3	1800 s	[46, 39, 40, 47, 172]	3.40 s
4	2400 s	[35, 33, 36, 35, 151]	3.94 s
5	3000 s	[40, 39, 40, 41, 172]	4.05 s
6	3600 s	[36, 37, 36, 42, 163]	3.88 s

The signal timing plans optimized for six iterations and the original signal timing plan are separately input into the signal controller via the VISSIM–COM interface. Based on the real-time evaluation results from VISSIM, the total delay time, total queue length, and total pollutant emissions for this intersection were obtained, as shown in Table 7. We observe substantial reductions in total delay, queue length, and pollutant emissions following the algorithm’s interventions.

**Table 7.** Multi-Objective Model Optimization Results.

Number of Optimizations	Total Delay (s)	Total Queue Length (m)	Total Emissions of Pollutants (g)
1	12,412	987	10,188
2	14,115	1145	12,804
3	13,897	1036	13,741
4	14,852	1287	11,568
5	15,963	1695	17,865
6	12,008	1448	14,890
Average	13,874.5	1266.3	13,509.3
Unoptimized	17,542	1647	15,984

In order to further visually compare the gap before and after optimization, we will make a standardized comparison between the indicators before optimization and the indicators after optimization, and plot a histogram, as illustrated in Figure 6. It can be observed that, after optimization using the single-point intersection signal control optimization model, the total delay at the intersection decreased by 21%, the total queue length decreased by 23%, and the total pollutant emissions decreased by 15%. The optimization results were notably significant, demonstrating the effectiveness of the multi-objective optimization model and the solving algorithm proposed in this paper.

**Figure 6.** Comparison Before and After Optimization of the Multi-Objective Model.

## 5. Conclusions

This paper aimed to reduce vehicle delay, queue length, and pollutant emissions at intersections. It established a multi-objective optimization model for single-point intersection signal timing, with intersection saturation, green light duration, and signal cycle as constraint conditions. During the solution process, the selection operator of the genetic algorithm was modified by directly preserving the fittest individual from the current generation as offspring. This ensured that the best solution in the current generation always remained the best solution throughout the evolutionary process. Furthermore, a VISSIM microscopic simulation system framework was developed, and within this framework, rolling optimization was performed at the intersection every 10 min. Finally, using an actual intersection as an example, the effects before and after optimization were compared. It was found that, after optimization using the multi-objective model, the total delay at the intersection decreased by 21%, the total queue length decreased by 23%, and the total pollutant emissions decreased by 15%. The optimization results were significant, demonstrating the effectiveness of the multi-objective optimization model and the solving algorithm proposed in this paper.

However, the proposed method is not free from limitations. Firstly, although the indicators of signal timing optimization include emissions, queuing time, etc., other indicators deserve to be explored. Secondly, there are many models of vehicle emissions, and this article does not analyze which model is more realistic. Finally, there are still many ways to solve the optimal solution of the objective function and, although genetic algorithm is beneficial, other methods are also worthy of further study.

In addition, there are still some problems to be further studied: (1) When formulating the signal timing optimization method, different indicators can be given different weights, and the multi-objective optimization model can be formulated in more detail. (2) The emission model can vary according to different road conditions and different vehicles. (3) The algorithm deserves further improvement and optimization, which will contribute more to the accuracy of the solution.

**Author Contributions:** Study conception and design: B.G. and S.Z.; model design and implementation: S.W. and Y.Z.; analysis and interpretation of results: D.W., B.G. and S.W.; draft manuscript preparation: B.G., Y.Z. and S.Z.; funding acquisition: B.G. and S.W. Validation, Writing—Review & Editing: D.W. and C.W. All authors have read and agreed to the published version of the manuscript.

**Funding:** This work was partly supported by the Scientific Research Project of the Education Department of Jilin Province (Grant No. JJKH20221020KJ) and the Qingdao Social Science Planning Research Project (Grant No. 2022-389).

**Data Availability Statement:** The data used to support the findings of this study are available from the corresponding author upon request.

**Conflicts of Interest:** Authors Shan Wang, Yu Zhao were employed by the Shanghai Urban Construction Design and Research Institute (Group) Co., Ltd. Author Shaoqi Zhang was employed by the company China FAW Group Co., Ltd. Authors Dongbo Wang, Chao Wang were employed by Bureau of Transportation and Construction, TEDA Administrative Commission. The remaining authors declare that the research was conducted in the absence of any commercial or financial relationships that could be construed as a potential conflict of interest.

## References

1. Baidu. China Urban Transportation Report. 2022. Available online: <https://jiaotong.baidu.com/cms/reports/traffic/2022/index.html> (accessed on 27 February 2023).
2. Fan, J.; Gao, K.; Xing, Y.; Lu, J. Evaluating the effects of one-way traffic management on different vehicle exhaust emissions using an integrated approach. *J. Adv. Transp.* **2019**, *2019*, 6248796. [CrossRef]
3. Frey, H.C.; Unal, A.; Roupail, N.M.; Colyar, J.D. On-Road Measurement of Vehicle Tailpipe Emissions Using a Portable Instrument. *J. Air Waste Manag. Assoc.* **2003**, *53*, 992–1002. [CrossRef] [PubMed]

4. Liu, L.; Wei, L. Research on Intersection Signal Timing Based on Multi-Objective Linear Combination. In Proceedings of the 2022 4th International Conference on Artificial Intelligence and Advanced Manufacturing (AIAM), Hamburg, Germany, 7–9 October 2022.
5. Li, Y.M. Research on Optimization of Pre-Signal Bus Priority Control at Intersections Based on Exhaust Emissions. Master's Thesis, Beijing Jiaotong University, Beijing, China, 2022.
6. Jiang, X.Y. Research on Intersection Traffic Control Strategies Combined with Environmental Analysis. Master's Thesis, North China University of Technology, Beijing, China, 2015.
7. Dong, W.H. Multi-Objective Optimization Research of Traffic Signal Timing Considering Emission Characteristics. Master's Thesis, Beijing University of Technology, Beijing, China, 2016.
8. Lyu, P.; Wang, P.; Liu, Y.; Wang, Y. Review of the studies on emission evaluation approaches for operating vehicles. *J. Traffic Transp. Eng.* **2021**, *8*, 493–509. [[CrossRef](#)]
9. Frey, H.C.; Zhang, K.; Roupail, N.M. Fuel Use and Emissions Comparisons for Alternative Routes, Time of Day, Road Grade, and Vehicles Based on In-Use Measurements. *Environ. Sci. Technol.* **2008**, *42*, 2483–2489. [[CrossRef](#)]
10. Li, Y.; Song, J.; Yang, J. A review on structure model and energy system design of lithium-ion battery in renewable energy vehicle. *Renew. Sustain. Energy Rev.* **2014**, *37*, 627–633. [[CrossRef](#)]
11. Liu, T.; Wang, Q.; Su, B. A review of carbon labeling: Standards, implementation, and impact. *Renew. Sustain. Energy Rev.* **2016**, *53*, 68–79. [[CrossRef](#)]
12. Brzezinski, D.J.; Enns, P.; Hart, C.J. *Facility Specific Speed Correction Factors*; US Environmental Protection Agency, Air and Radiation: Washington, DC, USA, 1999.
13. Saharidis, G.K.D.; Konstantzos, G.E. Critical overview of emission calculation models in order to evaluate their potential use in estimation of Greenhouse Gas emissions from in port truck operations. *J. Clean. Prod.* **2018**, *185*, 1024–1031. [[CrossRef](#)]
14. Costagliola, M.A.; Costabile, M.; Prati, M.V. Impact of road grade on real driving emissions from two Euro 5 diesel vehicles. *Appl. Energy* **2018**, *231*, 586–593. [[CrossRef](#)]
15. Li, Y.R.L. Analysis of Factors Affecting Motor Vehicle Emission Factors at Signalized Intersections. *J. Beijing Jiaotong Univ.* **2019**, *43*, 122–131.
16. Hernandez, J.A.; Al-Qadi, I.L.; Ozer, H. Baseline rolling resistance for tires' on-road fuel efficiency using finite element modeling. *Int. J. Pavement Eng.* **2017**, *18*, 424–432. [[CrossRef](#)]
17. Wang, H.; Al-Qadi, I.L.; Stanciulescu, I. Simulation of tyre-pavement interaction for predicting contact stresses at static and various rolling conditions. *Int. J. Pavement Eng.* **2012**, *13*, 310–321. [[CrossRef](#)]
18. Gastaldi, M.; Meneguzzer, C.; Giancristofaro, R.A.; Gecchele, G.; Della Lucia, L.; Prati, M.V. On-road measurement of CO<sub>2</sub> vehicle emissions under alternative forms of intersection control. *Transp. Res. Procedia* **2017**, *27*, 476–483. [[CrossRef](#)]
19. Haydari, A.; Zhang, M.; Chuah, C.-N.; Ghosal, D. Impact of Deep RL-based Traffic Signal Control on Air Quality. In Proceedings of the 2021 IEEE 93rd Vehicular Technology Conference (VTC2021-Spring), Helsinki, Finland, 25–28 April 2021; pp. 1–6.
20. Lyu, P.; Lin, Y.; Wang, Y. The impacts of household features on commuting carbon emissions: A case study of Xi'an, China. *Transportation* **2019**, *46*, 841–857. [[CrossRef](#)]
21. Pallavidino, L.; Prandi, R.; Bertello, A.; Bracco, E.; Pavone, F. Compilation of a road transport emission inventory for the Province of Turin: Advantages and key factors of a bottom-up approach. *Atmos. Pollut. Res.* **2014**, *5*, 648–655. [[CrossRef](#)]
22. Barth, M.; Malcolm, C.; Younglove, T.; Hill, N. Recent validation efforts for a comprehensive modal emissions model. *Transp. Res. Rec.* **2001**, *1750*, 13–23. [[CrossRef](#)]
23. Mensink, C.; De Vlieger, I.; Nys, J. An urban transport emission model for the Antwerp area. *Atmos. Environ.* **2000**, *34*, 4595–4602. [[CrossRef](#)]
24. Gao, Y.; Hu, H. Estimation of Exhaust Emissions from Queued Vehicles at Signal-Controlled Intersections Based on the Specific Power Method. *China J. Highw. Transp.* **2015**, *28*, 101–108.
25. Sun, X.F. Research on Emission Estimation Methods at Signalized Intersections under Vehicle-Road Cooperation. Master's Thesis, Beijing Jiaotong University, Beijing, China, 2016.
26. Liao, T.-Y.; Machemehl, R.B. Development of an Aggregate Fuel Consumption Model for Signalized Intersections. *Transp. Res. Rec.* **1998**, *1641*, 9–18. [[CrossRef](#)]
27. Liao, T.-Y. A fuel-based signal optimization model. *Transp. Res. Part D Transp. Environ.* **2013**, *23*, 1–8. [[CrossRef](#)]
28. Hongtao, B.X.X. Emission Analysis of Urban Road Intersection Organization Optimization Based on MOVES. *J. Chongqing Univ. Technol.* **2018**, *32*, 115–121.
29. Wu, M.Z. Study on Motor Vehicle Exhaust Emissions at Urban Indirect Left-Turn Intersections. Master's Thesis, Southwest Jiaotong University, Chengdu, China, 2020.
30. Bowen, Y.Z.Q. Traffic Signal Optimization Method Considering Low Emission and Low Delay. *J. South China Univ. Technol.* **2015**, *41*, 29–34.
31. Li, J.Z. Research on Traffic Signal Control Models and Optimization Methods for Low Pollution Emissions. Master's Thesis, South China University of Technology, Guangzhou, China, 2018.
32. Transportation Research Board. *Highway Capacity Manual*; Transportation Research Board, National Research Council: Washington, DC, USA, 2000.
33. Gazis, D.C.; Herman, R.; Potts, R.B. Car-following theory of steady-state traffic flow. *Oper. Res.* **1959**, *7*, 499–505. [[CrossRef](#)]

34. Jiang, X.C.; Pei, Y.L. Adaptive Signal Control Delay Model Based on Queueing Theory. *J. Traffic Transp. Eng. Inf.* **2008**, *3*, 66–70.
35. Wu, T.; Ma, N.; Zheng, S. Correlation analysis of signalized intersection saturation and delay. *Highw. Nat.* **2012**, *4*, 55–60.
36. Alhijawi, B.; Awajan, A. Genetic algorithms: Theory, genetic operators, solutions, and applications. *Evol. Intel.* **2023**, 1–12. [[CrossRef](#)]
37. Goldberg, D.E.; Holland, J.H. Genetic Algorithms and Machine Learning. *Mach. Learn.* **1988**, *3*, 95–99. [[CrossRef](#)]

**Disclaimer/Publisher’s Note:** The statements, opinions and data contained in all publications are solely those of the individual author(s) and contributor(s) and not of MDPI and/or the editor(s). MDPI and/or the editor(s) disclaim responsibility for any injury to people or property resulting from any ideas, methods, instructions or products referred to in the content.